

# A new method for volumetric measurement of orthodontically induced root resorption craters

Eugene K. M. Chan<sup>1</sup>,  
M. Ali Darendeliler<sup>1</sup>, Peter Petocz<sup>2</sup>,  
Allan S. Jones<sup>3</sup>

<sup>1</sup>Discipline of Orthodontics, Faculty of Dentistry, University of Sydney, Australia; <sup>2</sup>Department of Statistics, Macquarie University, Sydney, Australia; <sup>3</sup>Electron Microscopic Unit, University of Sydney, Australia

Chan EKM, Darendeliler MA, Petocz P, Jones AS. A new method for volumetric measurement of orthodontically induced root resorption craters. *Eur J Oral Sci* 2004; 112: 134–139. © Eur J Oral Sci, 2004

This method was designed to quantify root resorption on human premolar root surfaces induced by orthodontic forces by volume. Light (25 g) or heavy (225 g) orthodontic forces were applied to 20 first maxillary premolars in 10 human subjects. The contralateral teeth of the subjects served as controls. All teeth were extracted after 28 d of experimentation and prepared for imaging. A pair of stereo scanning electron microscopy (SEM) images ( $\pm 3^\circ$ ) of resorption craters was captured and imported into an image analysis software package. The images were aligned and grayscale depth maps of the craters were generated. Correction for errors due to residual tilt and curvature of the cementum surface using shading correction was performed. Thresholding was used to obtain a measure of both the cementum surface height and the average depth of the crater. The depth of the crater was the difference in these values. Crater volumes were obtained by multiplication of the average of this difference by area of the crater. Calibration of this volumetric measurement against standardized calculated known volumes on metallic rods showed good accuracy and reproducibility. In the experimental teeth, heavy forces caused threefold more resorption than light forces ( $P < 0.01$ ). There was also more root resorption evident in the experimental teeth compared with the control teeth in both the light and heavy force groups.

M. Ali Darendeliler, Discipline of Orthodontics, Faculty of Dentistry, The University of Sydney, Level 2, 2 Chalmers Street, Surry Hills, NSW 2010, Australia

Telefax: +61–2–93518336  
E-mail: adarende@mail.usyd.edu.au

Key words: root resorption; volumetric measurement; SEM; shading correction

Accepted for publication January 2004

Root resorption was first described by BATES in 1856 (1), and it was later correlated to orthodontics by OTTOLENGUI in 1914 (2). In orthodontics, for tooth movement to occur, a force with an appropriate magnitude is required to initiate a cascade of reaction locally which allows remodeling of the tooth supporting tissues. This remodeling process occurs as tissue resorption on the pressure side and tissue apposition on the tension side of the tooth socket. While forces that are too weak and inconsistent are insufficient to move teeth, forces that are too large are believed to cause excessive root resorption as an unwanted side-effect (3–5). Most studies investigating the magnitude of orthodontic forces affecting the degree of root resorption have been inconclusive. Being a three-dimensional (3-D) phenomenon, root resorption craters occurring on the curved surface or apex of the root of a tooth have been difficult to quantify. Previous research programs have studied these craters by measuring root shortening on radiographs (6–9), while others have quantified the extent of root resorption by two-dimensional (2-D) area measurements of these craters (10, 11). These studies have been inconclusive because of flaws detected in their methodology. The technical difficulty in obtaining an accurate 3-D analysis of the resorption craters have prevented the true understanding and implication of this phenomenon in its entirety (12). The aims of this study were to produce digital 3-D replicas of

root resorption craters and use these digital models to develop a new protocol for volumetric measurements of root resorption craters. Scanning electron microscope (SEM) was used to capture the images of the craters to allow the study of this subject in greater detail.

## Material and methods

A sample of 20 human first maxillary premolars from patients requiring at least bilateral first maxillary premolar extraction as part of their orthodontic treatment (Ethical approval: Project 5/98 Central Sydney Area Health Services Human ethics review committee, United Dental Hospital, NSW, Australia) was obtained. The teeth were randomly divided into two groups. On one side of the arch, buccally directed light (25 g) or heavy (225 g) tipping orthodontic force was applied to the teeth with a  $\beta$ -titanium molybdenum alloy (TMA; Ormco, Orange, CA, USA) cantilever springs spanning from the first molar to the first premolar on Speed brackets (Strite Industries, Cambridge, ON, Canada). The contralateral sides served as controls (0 g). The teeth were extracted by one operator after an experimental period of 28 d. They were then soaked for 10 min in a Milli-Q (deionized water) ultrasonic bath (Millipore, Bedford, MA, USA) to remove all traces of soft tissue fragments. The teeth were then carefully cleaned with a gauze swab to remove fragments of periodontal ligament.

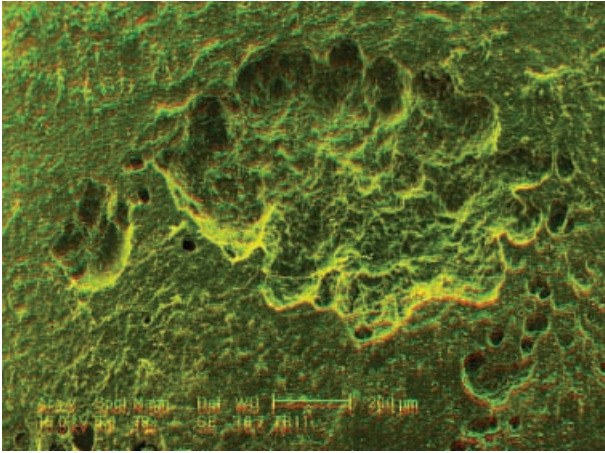


Fig. 1. A red–green anaglyph showing of a root resorption crater on the surface of root cementum.

They were then disinfected in 70% alcohol for 30 min, and each specimen was stored separately in Milli-Q at  $23 \pm 1^\circ\text{C}$  until time of experimentation, as described in a previous study (13). All specimens were mounted on a stainless steel diamond coated high-speed long shank chamfer bur secured with Glass ionomer cement (Transbond; 3M Unitek, St Paul, MN, USA) and bench dried for at least 48 h. The specimens were carbon coated (Edwards Coating System E306A) to a thickness of between 250 Å and 300 Å. They were then imaged using a XL30 SEM (Philips, Eindhoven, The Netherlands). A motorized rotating jig was created to enable all aspects of the sample to be studied in a full  $360^\circ$  angle via an external control without constant opening of the SEM chamber. This allowed total 3-D control of the teeth and enabled image capture at approximate zero degrees to the horizontal plane. In this way, the mesio-buccal, mesio-lingual, disto-buccal as well as the disto-lingual surfaces could be easily studied and craters in these regions would not be missed. Two SEM images of each crater were collected with introduction of a  $6^\circ$  tilt ( $\pm 3^\circ$ ) to produce a stereo pair of each crater. The images were all focused at the eucentric point with the SEM operated at 15 kV and spot size 5, which corresponds to a diameter of approximately 200 nm, and saved as TIFF images. The difference in parallax of each image was then used to generate the 3-D image of the crater. The root resorption craters were initially visualized using 3-D red–green stereo anaglyph coding (Fig. 1) to obtain a quick and simple qualitative assessment (AnalySIS Pro 3.1; Soft Image System, SIS, Münster, Germany). Images were first imported into the software as a matched pair (i.e.  $+3^\circ$  tilt and  $-3^\circ$  tilt) for each crater under examination. One image was then rendered in a red intensity scale while the other image in the pair was rendered in a green intensity scale. A single color composite image was then formed by superimposing the data from both images. Subsequent viewing of this anaglyph with a pair of red–green 3-D glasses results in visual depth cueing and generation of a 3-D visualization effect.

Quantitative measurement of the volume of the root resorption craters was undertaken using a SIS MACRO (macroinstruction, i.e. application specific programming language), based on the SIStereo imaging module. Using the image pair imported for anaglyph generation, a point of reference was selected in one of the images that would also be clearly visible in the second image. This point was usually a high-contrast particle at the edge of the crater. The soft-

ware uses this reference point to define a small region and then uses correlation to accurately align the images. Once aligned, the parallax difference allowed generation of a new 8-bit grayscale image in which depth differences were encoded as different gray values.

A technique known as shading correction, which has typically been used in microscopy to correct uneven illumination due to the curvature of the microscope field (14) was applied in this study to correct for the innate curvature of the surface of the sample. On the grayscale depth image, three widely spaced ‘hot-spots’, 20 pixels in diameter, were selected from the tooth surface. The average pixel values in these three selected areas was then used to define a correction plane for the entire image that removed the majority of the residual tilt bias due to curvature while maintaining the difference in the gradient of the pixels that encoded the crater depth information. In this way, the tilt of the image was corrected and the depth profile was generated (Fig. 2).

A 3-D mapping of the resorption crater was generated from the constructed depth profile. This allowed total interactive viewing of the crater from all directions. The morphology and topography of the craters could then be examined in greater detail in a natural context without having to use red-green anaglyph glasses. As a further enhancement of this visualization process, the crater could also be viewed in a continuous motion format using the flight simulation module of the software.

The corrected depth profile was further used to obtain volumetric measurements of the craters. The 2-D extent of the crater was determined by segmenting the corrected depth profile image using thresholding. Border particles were removed and holes filled using binary processing to ensure that the entire crater was included without any extraneous material. An initial threshold level was set so that surface height ( $x$ ) of the tooth cementum could be defined. A subsequent threshold was then applied to obtain the depth of the crater ( $y$ ), which was defined as the average of the depth encoded gray values within the 2-D extent of the crater. The difference between  $x$  and  $y$  was then determined as the average depth of the crater. The volume of each crater was then obtained by multiplying this value with the measured 2-D planar area (i.e. extent) of the crater. To eliminate any statistical variability, all craters were imaged four times and each pair of images were processed a further two times. There were hence eight replicate measurements obtained per crater.

This volumetric measuring method was calibrated against artificial indentations of known, calculated volumes made by a Vickers Microhardness tester Type M (Shimadzu, Tokyo, Japan) with a pyramidal indenter on two standard solid metal cylinders, brass and stainless steel. These rods were selected to match the size and dimensions of the human premolars; the metals were selected because of their high degree of hardness to prevent elastic deformation during the indentation process. The diamond pyramidal indenter of the Vickers indenter had a  $136^\circ$  inclusion angle. Thus, the volume of these indentations could be mathematically calculated using the formula

$$v = ah/3$$

where  $v$  is the volume,  $a$  is the base area of the pyramid and  $h$  is the height. Eight indentations were made on the maximum curvature and along the long axis of each rod. The calculated volumes were compared to the estimated volumes derived by measurement of the stereo images obtained from the SEM. The calculated and estimated volumes were measured eight times for each indentation (i.e.  $n = 64$ : eight replicates of eight indentations).

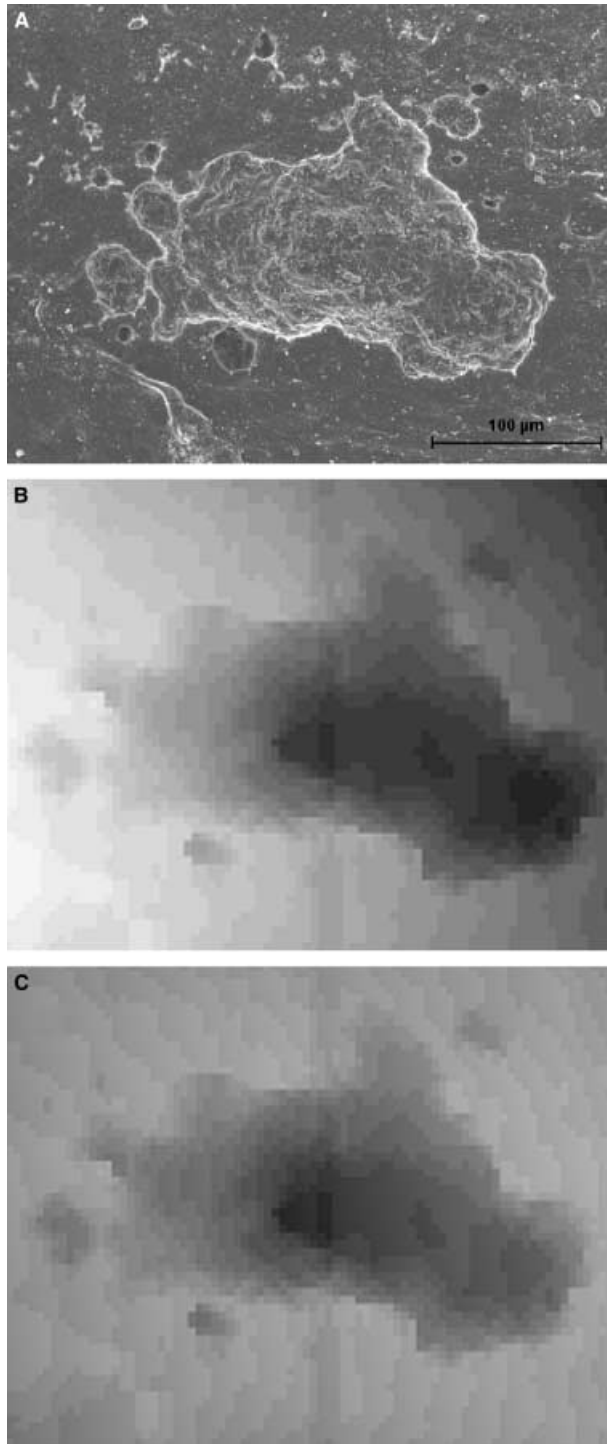


Fig. 2. Diagrams demonstrating (A) scanning electron microscopy image of crater, (B) preshading correction of 8-bit grayscale image, and (C) post-shading corrected image.

## Results

The initial visualization of the crater was obtained through generation of a red-green anaglyph. This anaglyph allowed a qualitative preliminary overview of the crater when viewed using a pair of red-green 3-D

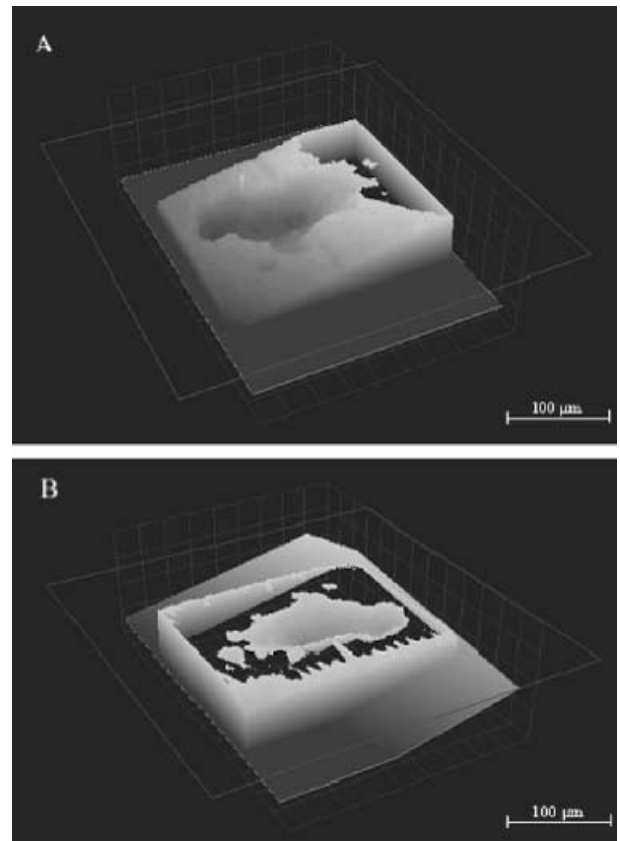


Fig. 3. Three-dimensional representation of crater (A) prior to shading correction, and (B) after shading correction.

glasses. When the crater was converted from the SEM stereo pair images to an 8-bit grayscale depth map image, a 3-D surface format of the crater could also be generated for visualization. With shading correction performed, the uneven illumination of the image resulting from the innate curvature of the sample was overcome and the efficacy of the shading correction of the crater was demonstrated (Fig. 3).

A further enhancement of the qualitative aspect of the images was obtained by uploading a series of consecutively captured images into a flight simulation module of the software. This not only allowed us to view the crater in 3-D but also allowed us to view it in dynamic motion from any desired direction (Fig. 4). This permitted real-time viewing of the crater at a high level of surface detail. The morphology and topography of the crater could be closely studied. Remnants of Sharpey's fiber insertions seen as dimples on the cementum surface and exposed dentinal tubules in the depth of the crater could be visualized.

Calibration of the stereo pair generated depth map volumes against microindentation volumes demonstrated a high level of accuracy and reproducibility for the measurement technique. For the 64 replicate indentation measurements on the brass rod, the mean calculated volume of the indentation correlated favorably with the mean volume estimated from the stereo pair measurements (Table 1). For the 64 replicate indentation

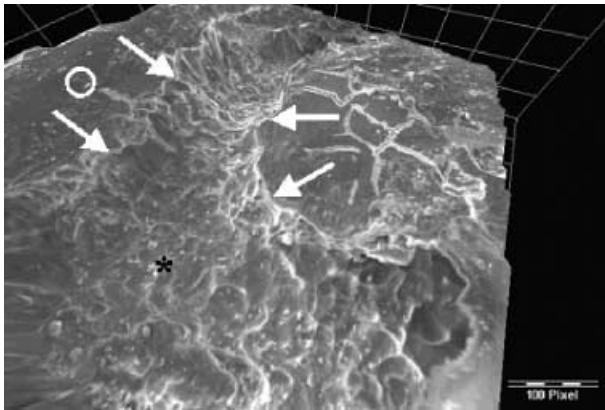


Fig. 4. Snapshot of flight simulator program with the three-dimensional replica of the crater. White arrows, edge of crater; \*, exposed dentinal tubules; O, remnants of Sharpey fiber insertions.

Table 1

Table showing mean calculated and estimated volumes of the 64 replicate indentations on the brass and stainless steel rods

	Type of material	n	Mean	SD	SEM
Calculated volume ( $\mu\text{m}^3$ )	Brass	64	8663.47	441.17	55.15
	Stainless steel	64	8160.49	414.55	51.82
Estimated volume ( $\mu\text{m}^3$ )	Brass	64	8973.13	745.60	93.20
	Stainless steel	64	8281.02	1355.14	169.39

measurements on the stainless steel rod, the mean calculated volume of the indentation again correlated favorably with the mean volume estimated (Table 1). Using *t*-test for the equality of means, these figures corresponded to *P*-value < 0.001 in both cases.

In the other part of the study examining the sample of 20 teeth (five light force controls, five light force experimental, five heavy force controls and five heavy force experimental), in the experimental groups, the mean volume of resorption in the heavy force group was  $898.61 \times 10^5 \mu\text{m}^3$  compared with  $291.69 \times 10^5 \mu\text{m}^3$  in the light force group (*P* < 0.01). This corresponds to about threefold more resorption by volumetric measurement in the heavy group compared with the light force group. There was also more root resorption evident in the experimental teeth compared with the control teeth in both the light and heavy force groups (Table 2). Using a paired *t*-test, the *P*-value was < 0.01 in both cases.

## Discussion

No previous studies have made attempts at quantifying the extent of root resorption by 3-D volumetric measurement of the resorption craters. Microanalysis of 3-D ultra-structures and visualization of the sample has, however, always been a challenge owing to various technical difficulties. In this study, root resorption craters examined under SEM and reconstructed as a 3-D

Table 2

Table showing volumetric measurements of craters in control and experiment, light and heavy groups

Force	Control/ experimental	Mean volume ( $\times 10^5 \mu\text{m}^3$ )	SEM
Light	Control	4.21	4.04
	Experimental	291.69	90.49
Heavy	Control*	0.00	0.00
	Experimental	898.61	353.21
Total	Control	2.10	2.02
	Experimental	557.21	168.34

\*No craters were detected in the control teeth of the heavy force group.

red-green anaglyph allows for quick overviews and clear visualization of the extent of the destruction of the cementum of the root surface.

Although great care was taken to ensure that samples were mounted horizontally and that images were collected from directly above each crater by axial rotation using the motorized jig, additional spatial corrections were required to ensure accuracy of the measurement data. For the larger craters in particular, some residual tilt was inherent in the images of the craters due to the fact that the tooth surface was not totally flat, but had a curvature that varied over both the horizontal and vertical dimensions. This curvature of the cementum, if uncorrected in the depth image, would have resulted in inaccuracies in subsequent volume measurements.

The shading correction technique applied in this instance to correct for residual tilt and surface curvature proved to be simple and effective without requiring undue complexity of processing. By using the average of the pixels in three selected background areas a simple plane was defined which allowed the grayscale depth values to be corrected for gross errors, particularly along the axial length of the tooth surface where curvature was higher. A further improvement in measurement accuracy could be obtained by the use of a non-linear correction surface rather than a simple plane; however, this would require substantially more complex image processing to define the exact curvature at any given background point. Given the relatively minor gain in accuracy that such a method would achieve, the added complexity does not, in our opinion, seem warranted for our particular studies. It would, however, be worthy of consideration for studies where the surface topography was more complex.

The added advantage of this 3-D analysis was that the consecutively captured images could be uploaded into a flight simulation module and allows the craters to be visualized from a different perspective again. Coupled with the capabilities of viewing the red-green anaglyph in a 3-D flight simulation as well, the true understanding of the extent of root resorption is enhanced. An in-depth examination of the topography and morphology of resorption craters can be performed and documented.

This study of 20 teeth obtained from a prescribed human sample allowed us to demonstrate that

volumetric analysis could be used to measure the extent of root resorption in artificially induced root resorption craters. It was evident that there was more root resorption in the heavy compared with the light group. It was also demonstrated that there was more root resorption evident in the experimental group compared with the controls in both the light and heavy groups. These findings are consistent with previous studies performed in both animal and human models (15–17).

SCHWARTZ (18) first proposed the pressure-tension theory in the biology of tooth movement in 1932. He suggested that the optimal force level for tooth movement should be between  $7 \text{ g cm}^{-2}$  and  $26 \text{ g cm}^{-2}$  of root surface area. As reported by JEPSEN (19), the amount of surface area of a premolar tooth was  $2.34 \pm 0.33 \text{ cm}^2$ . Hence, in the present study, 25 g was selected as the light force. A triple exponential increase was selected for the heavy force at 225 g. The larger amount of resorption measured in the heavy force group could be explained by the presence of a larger compressive force of the tooth–bone interface. It has also been reported that at high level of orthodontic forces, undermining resorption of the alveolar bone occurs in order for tooth movement to proceed (20). This allows a larger cascade of cellular activity at the tooth–bone interface and may contribute to increased root resorption of the tooth cementum.

In the present study, even though the premolars were carefully selected to exclude any local or systemic predisposition to resorption, resorption craters were still evident in small quantities in the controls of the light force group. This demonstrated that resorption could be a naturally occurring physiological phenomenon (21).

Being a new technique, the calibration of this volumetric measuring exercise was essential. Metallic rods with a high degree of hardness were chosen to prevent non-uniform elastic deformation during indentation. Cylindrical rods were used to mimic the actual dimensions of human premolars. The mathematically calculated volume of the pyramidal indentations, when compared with the estimates obtained by the analysis software demonstrated high levels of accuracy and reproducibility.

Previously, 3-D reconstruction of an irregularly shaped, open crater would involve embedding the specimen in resin. Careful thin sections were made and subsequently imaged with a transmission electron microscope. The images could then be pieced together with software to study the sample in three dimensions. This process is tedious and technique sensitive. There exist innate problems, such as some samples not being suitable to embed in resins. In addition, physical sectioning also has problems associated with loss of material due to the thickness of the cutting kerf, which is usually of the order of  $300 \mu\text{m}$ . Furthermore, once embedded and sectioned, the sample would not be intact for any further experimentation.

In this investigation, after volumetric analysis was performed on these samples, they were then embedded and sectioned. A further study with these samples looked at the mineral content and composition of the root cementum with an electron probe. This would not be possible with the old technique.

The technique presented in this paper has greatly facilitated ongoing studies of root resorption in relation to orthodontic procedures. It has overcome the limitations associated with physical sectioning and has the advantage of being rapid and accurate. In addition, the combination of stereo-imaging and modern digital analysis has resulted in a method that has a high visual context that allows researchers to have visual checking against quantitative data. The craters could then be measured for quantitative comparison, and finally the 3-D nature of this data allowed a dynamic visualization to be generated from which the morphology of the craters to be examined in greater detail.

This study demonstrated that an accurate 3-D volumetric measurement of root resorption craters in a controlled human model could be achieved. The accuracy of this measurement has also been verified (22). Based on this notion, a larger sample size would need to be collected to document further the effects of magnitude on the extent of root resorption in human premolars.

*Acknowledgments* – We thank Dr I.J. Kaplin and the staff of the Electron Microscopic Unit (EMU, University of Sydney, Australia) for their invaluable assistance in preparation of this manuscript.

## References

- BATES S. Absorption. *Br J Dent Sci* 1856; **1**: 256.
- OTTOLENGUI R. The physiological and pathological resorption of tooth roots. *Item Interest* 1914; **36**: 332–362.
- KING GJ, FISCHLSCHWEIGER W. The effect of force magnitude on extractable bone resorptive activity and cemental cratering in orthodontic tooth movement. *J Dent Res* 1982; **61**: 775–779.
- KVAM E. SEM of tissue changes on the pressure surface of human premolars following tooth movement. *Scand J Dent Res* 1972; **80**: 357–368.
- STOREY E, SMITH R. Force in orthodontics and its relation to tooth movement. *Aust J Dent* 1952; **56**: 11–18.
- HOLLENDER L, RONNERMAN A, THILANDER B. Root resorption, marginal bone support and clinical crown length in orthodontically treated patients. *Eur J Orthod* 1980; **2**: 197–205.
- SAMESHIMA GT, ASGARIFAR KO. Assessment of root resorption and root shape: periapical vs panoramic films. *Angle Orthod* 2001; **71**: 185–189.
- LYDIATT DD, HOLLINS RR, PETERSON G. Multiple idiopathic root resorption: diagnostic considerations. *Oral Surg Oral Med Oral Path Oral Radiol Endod* 1989; **67**: 208–210.
- MENAB S, BATTISTUTTA D, TAVERNE A, SYMONS A. External root resorption following orthodontic treatment. *Angle Orthod* 2000; **70**: 227–232.
- ACAR A, CANYUREK U, KOCAAGA M, ERVERDI N. Continuous vs. discontinuous force application and root resorption. *Angle Orthod* 1999; **69**: 159–164.
- BARBER AF, SIMS MR. Rapid maxillary expansion and external root resorption in man: a SEM study. *Am J Orthod* 1981; **79**: 630–652.
- CHAN EKM, DARENDELILER MA, PETOCZ P. Exploring the third dimension in root resorption. (Submitted for publication). *Orthod Craniofac Res* 2004; (in press).
- MALEK S, DARENDELILER MA, SWAIN MV. Physical properties of root cementum: Part I. A new method for 3-dimensional evaluation. *Am J Orthod Dentofac Orthop* 2001; **120**: 198–208.
- RUSS JC. *Computer-assisted microscopy: the measurement and analysis of images*. New York: Plenum Press, 1990.
- HARRY MR, SIMS MR. Root resorption in bicuspid intrusion: a scanning electron microscopic study. *Angle Orthod* 1982; **52**: 235–258.

16. KVAM E. SEM of human premolars following experimental tooth movement. *Trans Europ Orthod Soc* 1972; 381–391.
17. DELLINGER EL. A histologic and cephalometric investigation of premolar intrusion in the *Macaca speciosa* monkey. *Am J Orthod* 1967; **53**: 325–355.
18. SCHWARTZ AM. Tissue changes incidental to orthodontic tooth movement. *Inter J Orthod* 1932; **18**: 331–352.
19. JEPSEN A. Root surface measurement and a method for X-ray determination of root surface area. *Acta Odontol Scand* 1963; **24**: 35–46.
20. PROFFIT WR. The biologic basis of orthodontic therapy. In: *Contemporary Orthodontics*. 3rd edn. St Louis, MO: CV Mosby, 2000; 296–325.
21. HENRY JL, WEINMANN JP. The pattern of resorption and repair of human cementum. *J Am Dent Assoc* 1951; **42**: 270–290.
22. CHAN EKM, DARENDELILER MA, JONES AS, KAPLIN IJ. A calibration method used for volumetric measurement of orthodontically induced root resorption craters. *J Biomed Eng* 2004; (in press).